mathematics

MDPI

Article

Human-Machine Function Allocation Method for Submersible Fault Detection Tasks

Chenyuan Yang [1,†], Liping Pang [1,†], Wentao Wu [2] and Xiaodong Cao [1,3,*]

[1] School of Aeronautic Science and Engineering, Beihang University, No. 9, South Third Street, Higher Education Park, Beijing 102206, China; by2105512@buaa.edu.cn (C.Y.); pangliping@buaa.edu.cn (L.P.)
[2] Department of Civil and Natural Resources Engineering, University of Canterbury, Christchurch 8041, New Zealand; wentao.wu@canterbury.ac.nz
[3] Tianmushan Laboratory, Hangzhou 311115, China
* Correspondence: caoxiaodong@buaa.edu.cn; Tel.: +86-188-0019-6168
† These authors contributed equally to this work.

Abstract: The operation and support (OS) officer is responsible for buoyancy regulation and fault detection of onboard equipment in the civil submersible. The OS officer carries out the above tasks through the human-machine interface (HMI) of a submersible buoyancy regulation and support (SBRS) system. However, the OS officer often faces uneven task frequency produced by fault tasks, which leads to an unbalanced mental workload and individual failures. To address this issue, we proposed a human-machine function allocation method based on level of automation (LOA) taxonomy and submersible task complexity (STC), aimed at improving human-machine cooperation in submersible fault detection tasks. Based on this method, we identified the LOA2 as the optimal human-computer function allocation scheme. In this study, three measurement techniques (subjective scale, work performance, and physiological status) were used to test 15 subjects to validate the effectiveness of the proposed optimal human-machine function allocation scheme. The GAMM test results also indicate that the proposed optimal human-machine function allocation scheme (LOA2) can improve the work performance of the operating system officials under low or high workloads and reduce the subjective workload.

Keywords: human-machine function allocation method; level of automation; task complexity; workload; submersible

MSC: 03D15

Citation: Yang, C.; Pang, L.; Wu, W.; Cao, X. Human-Machine Function Allocation Method for Submersible Fault Detection Tasks. *Mathematics* **2024**, *12*, 3615. https://doi.org/10.3390/math12223615

Academic Editors: Biao Lu and Minnan Piao

Received: 25 September 2024
Revised: 13 November 2024
Accepted: 19 November 2024
Published: 19 November 2024

1. Introduction

Submersibles are an indispensable means of transportation to enter the deep sea for scientific research and investigation [1]. Among them, the operational deep-dive manned submersibles have become an important underwater vehicle in many categories and have provided strong technical support for the development of the international deep-sea industry [2]. As one of the important positions of the submersible, the submersible operation and support officer (OS officer) plays an important role in the submersible mission. Understanding and optimizing the workload (WL) of an OS officer is of great significance for preventing occupational diseases, guarding against fatigue, reducing human error, and improving the safety of diving.

It was found from our actual investigation that due to the complexity and unpredictability of the underwater environment, the OS officer of a submersible often faces unbalanced WL in the process of performing tasks in the deep sea. It is well known that there is an inverted U-shaped relationship between WL and system safe operation [3]. Excessive WL will not only cause the operator to appear physiologically stressed but also affect the sustained attention and working memory of the operator [4,5]. Especially in

emergencies, when the received information exceeds the processing capacity of the operator, they often respond to stimuli with a delay [6]. When the WL is too low, it is not enough to maintain situational awareness of the operator, and it will affect the response time [7]. Therefore, the unbalanced WL faced by an OS officer will affect the working efficiency and safety performance of the overall human-machine system [8].

Although the implementation of automation can reduce the WL of human operators, it also introduces certain challenges. First, it changes the role of the operator from that of a "performer" to that of a "supervisor". Second, the reduction in WL can result in a loss of situational awareness among operators [9]. Both of these phenomena can lead to a series of out-of-the-loop (OOTL) problems, such as operator complacency, reduced levels of monitoring, and degradation of operational skills [10,11]. Furthermore, as the level of automation (LOA) increases, the "lumberjack" phenomenon may emerge, meaning that when automation fails, greater human reliance on high levels of automation can lead to greater performance problems [12]. Therefore, a human-centered, rational allocation of functions is important to improve the overall human-machine collaboration performance.

The core aspect of human-machine interaction activities is the allocation of functions between humans and machines. The men are better at and machines are better at (MABA-MABA) list proposed by Fitts marked the beginning of research into human-machine function allocation [13]. The goal was to identify the strengths and limitations between humans and machines by comparing their relative capabilities, and then to determine the optimal division of responsibilities. However, the Fitts list has been criticized by many scholars for its inability to apply decisions to the design environment in an efficient and timely manner, its lack of iterative nature, and its failure to take into account the dynamic flow of information that affects the operator's understanding of the work state [14,15].

To provide a more effective basis for engineering design in the operational environment, Sheridan and Verplank introduced the automation level scale in 1978, which formed the original LOA taxonomy [16]. However, Wickens [17] pointed out that the Sheridan and Verplank scales were only applicable to automated decision recommendation functions and did not consider the impact of automation on the entire phase of human information processing. As a result, Endsley and Kaber [18] proposed an LOA taxonomy, applicable to a wide range of psychomotor and cognitive tasks. This taxonomy includes various schemes for the assignment of generic control system functions. Parasuraman et al. [19] proposed an automation type and automation level approach with more generality based on the information processing model (Wickens) [20]. This approach applies four stages of human information processing to automated systems: information filtering, information integration, action selection, and action implementation. The automation types and automation level approach provides greater generality and allows for useful function allocations between humans and machines. Moreover, it enables the continuous adjustment of LOA to optimize the performance of human-machine systems, making it a widely accepted taxonomy among scholars [17,21–23].

LOA taxonomy can provide designers with different LOAs to choose from, but extensive research has shown that the improvement in performance resulting from automation occurs at the mid-level of LOA [24–26]. At this level, operators shift from operational control to supervisory control, leading to reduced WL and psychological stress, as well as mitigated first failure effects [24,27].

Although LOA taxonomy provides a method for describing the LOA, this method is only a qualitative evaluation method. To develop a more reasonable and scientific human-machine function allocation strategy, this paper further used a quantitative evaluation method to measure the task complexity under different LOAs.

At present, there are related kinds of literature to quantify the task complexity. Ha et al. [28] developed a method to assess the step complexity (SC) of emergency operating procedures based on entropy measures used in software engineering. It is mainly composed of three sub-complexities: step logic complexity, step size complexity, and step information complexity and confirmed that the estimated SC values are generally consistent with the

NASA-TLX score and step performance time data. Zheng et al. [29] proposed the task complexity in flight (TCIF) method based on the SC method, which not only considers the task complexity during the task process but also quantitatively evaluates the human–computer interaction behavior. TCIF combines the four sub-complexities into one index value, and the TCIF results are experimentally verified to be consistent with the Bedford score and heart rate variability. Therefore, task complexity can effectively quantify the WL of subjects. Combined with the task characteristics of the submersible OS officer post, this study proposed a submersible task complexity (STC) method based on the TCIF method.

A human-machine function allocation method based on LOA taxonomy and STC was proposed in this study. This method first utilizes the LOA taxonomy to set different LOAs for specific work scenarios. Next, it uses the STC method to calculate the human-machine interaction complexity in each LOA work scenario. By comparing the complexity of human–machine interaction under different LOAs, we can determine the optimal human-machine function allocation scheme. The method proposed by this research institute is different from traditional functional allocation methods, as it integrates subjective and objective evaluations. To prove that the proposed human-machine function allocation method can optimize the work performance and WL of OS officers under an unbalanced WL, the relevant experimental verifications were carried out in this study.

2. SBRS System

In a submersible, the OS officer monitors and controls six subsystems by the human-machine interface (HMI) of the submersible buoyancy regulation and support (SBRS) system. Six subsystems consist of a submersible attitude control system (SACS), a submersible ups and downs control system (SUDCS), an equipment management system (EMS), an air conditioning system (ACS), an atmospheric composition processing system (ACPS), and a fire protection system (FPS). Taking the interface of SACS and ACS as an example, Figure 1 shows the HMIs and task operation process of SACS and ACS in the SBRS system simulator.

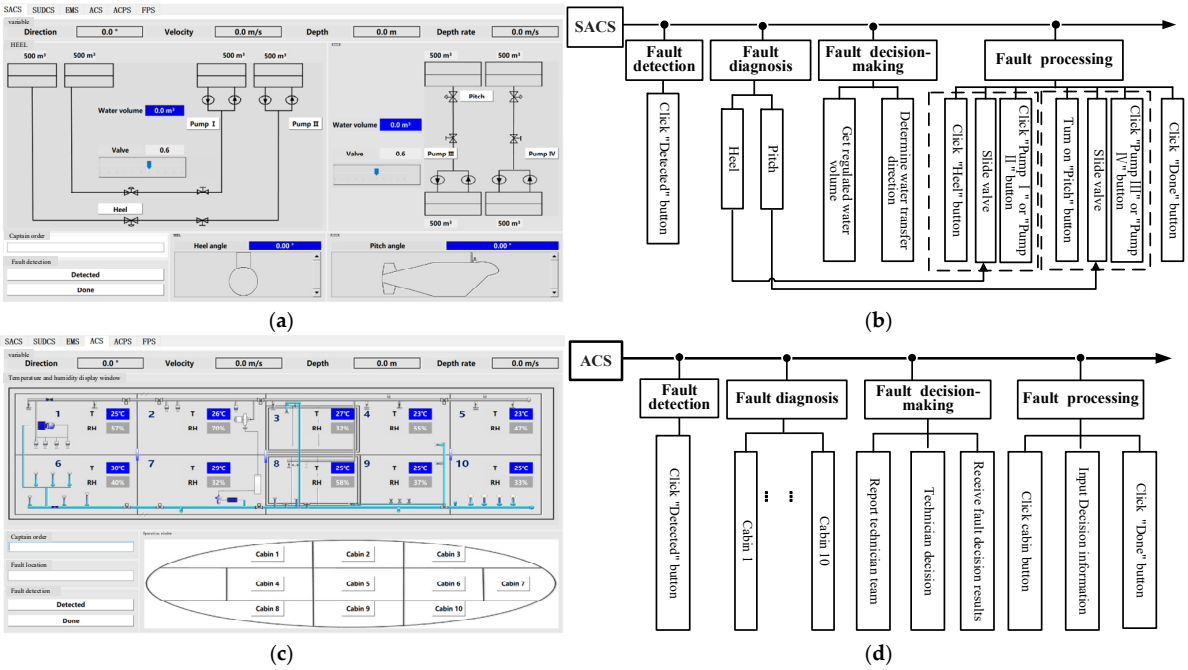

Figure 1. HMIs and task process of SBRS tasks. (**a**) SACS task HMI; (**b**) SACS task operation process; (**c**) ACS task HMI; (**d**) ACS task operation process.

The tasks to operate the SBRS system consists of primary and secondary tasks.

(1) Primary tasks (Buoyancy regulation tasks)

The primary tasks of OS officer are to operate the SACS and the SUDCS, which maintain the performance of the submersible buoyancy regulation. The primary tasks concern the safety of submersibles, hence they are high-priority tasks. Due to the change in seawater density, the inclination angle of submersibles often changes gradually during underwater navigation. The primary tasks of OS officers are to continually monitor the attitude and make any adjustments necessary to avoid overturning during the whole navigation.

Figure 1b shows the operational process of the SACS task. First, when OS officers observe an abnormality in the SACS interface, they click the "Detected" button. Second, they diagnose the fault as "Heel" or "Pitch". Then, they obtain the water regulation value and determine the direction of regulation. Finally, they click the "Pump" button, slide the valve, and click the "Heel" or "Pitch" button. After adjustment, they click the "Done" button.

(2) Secondary tasks (Fault detection tasks)

The secondary tasks of OS officers are to detect possible faults occurring in the EMS, the ACS, the ACPS, and the FPS. These fault detection tasks are low-priority tasks. After observing abnormal variation by human patrol inspection or alarm information from the automation system, the OS officer performs the fault diagnosis task. The OS officer needs to find the fault location in the corresponding system interface, judge the fault status, and finally make the processing decision.

Figure 1d shows the operational process of the ACS task. First, when OS officers observe an abnormality in the ACS interface, they click the "Detected" button. Second, they diagnose the faulty cabin. Then, they report the technical team's fault information via phone outside the interface, wait for the team's decision, and receive the decision information. Finally, they click on the cabin button, input the decision information, and click the "Done" button.

3. Human-Machine Function Allocation Method

Under normal conditions, the attention of the OS officer is mainly focused on performing primary tasks. At this time, the occurrence frequency of secondary tasks is low, and the WL of the OS officer is low. However, the increase of the detected fault frequency will lead to competition for attention resources. The OS officer not only deals with daily high-priority tasks but also allocates attention resources to handle low-priority tasks. This inevitably leads to a sharp increase in the WL. Therefore, based on the information processing model and submersible task complexity, this paper discusses a human-machine function allocation method mainly for secondary tasks to help balance subject WL and improve fault detection performance.

3.1. LOA Taxonomy

The four cognitive stages of individuals can characterize different information processing behaviors. Parasuraman et al. [19] proposed an automated level allocation based on these stages, which includes information filtering, information integration, action selection, and action implementation. However, these cognitive stages are not entirely independent of each other. The distinction between information filtering and information integration can be confusing, so this paper merges information filtering and information integration into a single stage. Figure 2 clearly illustrates the various stages of information processing for an OS officer.

(1) Information filtering and integration (fault detection and diagnosis)

The OS officer is primarily responsible for monitoring the primary task interface while also being able to quickly detect and diagnose any faults that may arise in secondary tasks. To accomplish this, the OS officer uses visual patrol inspection to gather information from the HMI and perceive faults in the EMS, ACS, ACPS, or FPS. However, the short-term impact of these fault occurrences can render the OS officer ill-prepared to respond quickly, which negatively impacts work performance. Once a fault is detected, the OS

officer integrates and infers information by combining working memory with retrieved information. Specifically, the OS officer identifies a specific fault by assessing whether the parameters are within reasonable ranges. To obtain specific fault diagnosis information and analyze fault point error information, the OS officer inspects the corresponding HMI. It should be noted that each fault detection task interface contains ten potential fault points, which can diminish visual search ability and increase WL for the OS officer.

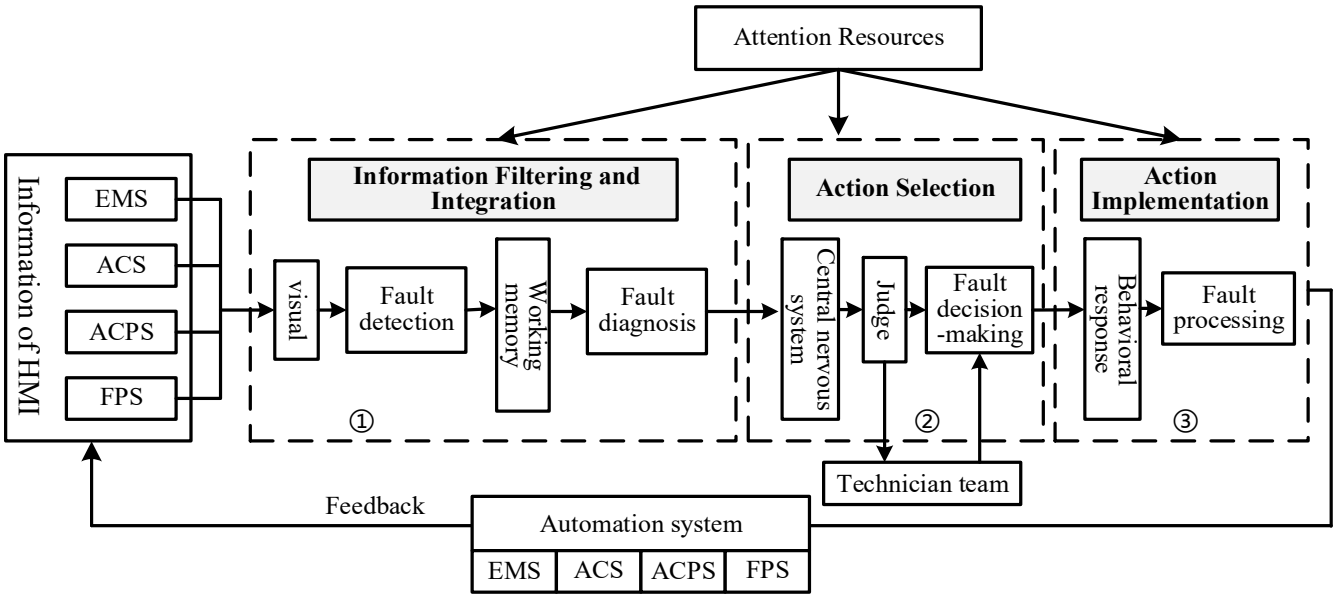

Figure 2. OS officer information processing stage.

(2) Action selection (fault decision-making)

In the second stage of fault decision-making, there is a team of professional technicians to support the OS officer making decisions after the fault diagnosis operation. The OS officer only needs to report the detected fault to the technicians of the corresponding system and await the failure decision result.

(3) Action implementation (fault processing)

The final stage is fault processing. After the fault resolution is determined in stage 3, the OS officer clicks on the corresponding faulty compartment and enters the fault decision result through HMI.

Through analysis of the three cognitive stages of the OS officer, it can be concluded that the selection and implementation of behavior must be carried out by the OS officer. As a result, this study places particular emphasis on the automation of information filtering and the integration stage, which is presented in Table 1.

Table 1. Task stage and LOA taxonomy of OS officer.

Information Processing Stage	Task Stage	LOA	Automation Implementation
Information filtering and integration	Fault detection and diagnosis	1	Machine locates the fault interface. OS officer diagnoses fault location and fault information.
		2	Machine locates the fault interface and prompts for the fault location and fault information.
		3	Machine pushes the specified fault interface and fault location directly to OS officer.

3.2. Submersible Task Complexity

Among the three LOAs mentioned above, the complexity of the OS officer operational tasks varies, and the corresponding WL also differs. In 1948, Shannon [30] introduced the concept of information entropy, defining it through probability distributions in probability theory and viewing information as quantifiable and uncertain events. The entropy measurement method was adopted to evaluate the task complexity based on the program control graph [28,31]. Mowshwitz [32] defined two types of entropy measures for graphs: first-order entropy for logical regularity and second-order entropy for the level of program control graphs. A higher entropy value corresponds to greater graph complexity. The entropy measurement method is shown in Equation (1):

$$H = -\sum_{i=1}^{N} p(A_i) \log_2 p(A_i) \quad (1)$$

where H is the entropy value; N is the number of node types; $p(A_i)$ is the probability of a node of class A_i; $-\log_2 p(A_i)$ is the information entropy of nodes of class A_i. Therefore, the graph information entropy is obtained by multiplying the information entropy of each node in the graph with its probability of occurrence and summing them up.

Multi-interface and multi-task features increase the HMI complexity. To analyze the task features of the SBRS system, a submersible task complexity (STC) method is set up in this paper referring to the task complexity in flight (TCIF) method [29]. The STC method can calculate four sub-complexities: actions logic complexity (ALC), actions size complexity (ASC), interface information interaction complexity (IIIC), and interface control behavior complexity (ICBC).

The ALC and the ASC of the task derived from the actions control graph describe the logical sequence and the number of required actions during task processing [29]. The HMI is the primary communication channel between the operator and the SBRS system. The complexity and diversity of HMI compete for the attention of operators [33]. During the processing of the fault detection task, the operator needs to pay attention to the primary tasks while also handling the secondary tasks. This multi-interface information interaction leads to operator overload. The IIIC includes the complexity of information interaction between the operation behavior and the interface systems and is calculated by the interface information interaction graph. The ICBC is calculated by the interface control behavior graph. The four complexity values can be combined into one indicator, namely the STC indicator, as shown in Table 2.

Table 2. Complexity, cause, graph, and entropy [29].

Complexity	Cause of Formation	Graph	Entropy Measure
ALC	Logical sequence of required actions	Actions control graph	Second-order entropy
ASC	The number of required actions	Actions control graph	First-order entropy
IIIC	HMI-interface information interaction	Interface information interaction graph	Second-order entropy
ICBC	HMI-interface control behavior	Interface control behavior graph	Second-order entropy

Taking the ACS task as an example, the calculation process of task complexity is described in Appendix A. Similarly, the task complexity values of other fault detection tasks in the EMS, the ACPS, and the FPS are calculated and summarized in Table 3.

Table 3. STC of fault detection tasks at different LOAs.

LOA	STC				
	EMS	ACS	ACPS	FPS	Average
LOA1	1.751	1.823	1.857	1.800	1.808
LOA2	1.504	1.617	1.643	1.587	1.587
LOA3	1.396	1.527	1.554	1.493	1.492

After analysis of the data, Table 3 shows that the STC decreases as the LOA increases. However, the improvement of LOA2 versus LOA1 (12.22%) task complexity was more significant compared to LOA3 versus LOA2 (5.99%).

3.3. Human-Machine Function Allocation Seclection

After analyzing the task characteristics of different cognitive stages in the SBRS task, it was determined that the OS officer should carry out operations during the action selection (fault decision-making) and action implementation (fault handling) stages. Human-machine collaboration could be conducted during the information filtering and integration stage (fault detection and diagnosis). Therefore, this study proposed three LOAs to target the information filtering and integration stage of the OS officer.

To clarify the rationality and effectiveness of different LOAs, we further quantified the task complexity of the secondary tasks of the OS officer under three LOAs. The results showed that the improvement in task complexity was more significant for LOA2 versus LOA1 (12.22%) compared to LOA3 versus LOA2 (5.99%). In addition, there was an interaction between the processing of primary and secondary tasks in the multi-interface tasks. For the LOA3, using an automatic pop-up interface for the secondary tasks may interrupt the process of OS officers handling the primary tasks, which is more frequent under HWL. Considering the complexity of the underwater work environment and balancing the benefits of automation and the impact of OOTL issues, this experiment chose LOA2 as the optimal human-machine function allocation. Figure 3 illustrates the human-machine function allocation developed for the submersible fault detection tasks.

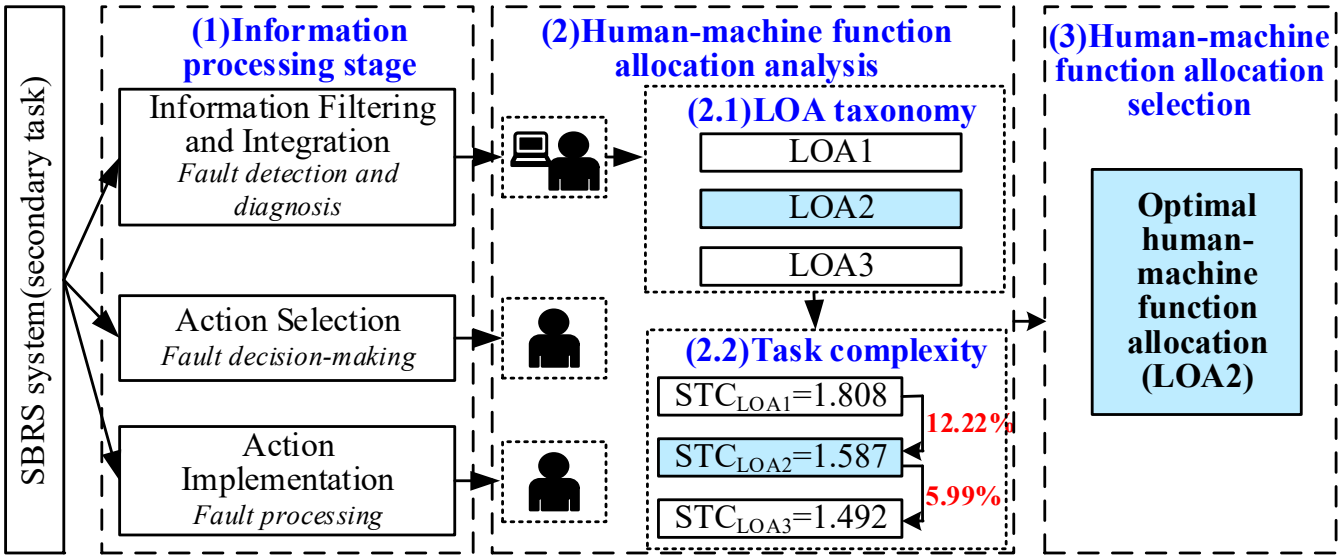

Figure 3. Human-machine function allocation for submersible fault detection tasks.

4. Experiment Methods

4.1. Subjects

Fifteen subjects ranging in age from 20 to 43 years (29.25 ± 7.58 years) were recruited to participate in this SBRS task experiment. Among all the subjects, one subject had a submersible work background, and six subjects had a science and engineering background. Subjects were healthy, right-handed, with normal or corrected vision, and a normal electrocardiogram. Before the formal experiments, the subjects received a two-week task training to fully familiarize themselves with the SBRS task operation under all conditions. After training, the operational accuracy of all subjects reached over 80%.

During participating in the task experiments, the subjects slept adequately, had a good mental state, and did not drink stimulant substances such as caffeine and alcohol. And no drug was taken before or during the experiment. All subjects completed the test without dropping out and received financial compensation after the experiment ended.

4.2. Experimental Design

4.2.1. Inpendent Variables

The primary purpose of the experiment was to test the effectiveness of the proposed LOAs in improving the WL and work performance of OS officers. Two types of WL tests were conducted: low workload (LWL) and high workload (HWL). The number of task events triggered during the tests was based on their frequency in the multi-attribute task battery (MATB) [34], as shown in Table 4. Each subject completed three LOAs (LOA1, LOA2, and LOA3) under LWL and HWL.

Table 4. Number of events triggered by various task types during the test.

Workload	Task Type			Test Duration /min
	Primary Task	Secondary Task	Total Task	
LWL	0	4	4	10
HWL	12	24	36	10

4.2.2. Dependent Variables

Direct (subjective scales) and indirect (work performance and ECG indicators) dependent variables were used to measure the LOAs under different WLs.

(1) Subjective scales

NASA-TLX and Bedford scales were mainly used to evaluate the subjective WL of subjects in this study [35]. NASA-TLX is a multi-dimensional and subjective technique for evaluating WL, which consists of two phases [36]. In the scoring stage, subjects choose an appropriate score (1–21) for each dimension to evaluate their status. In the weighting stage, the weight of each factor is defined by comparing the importance of all factors. Overall WL values of NSAS-TLX are divided into five categories [37]. Subjects were instructed to self-report their subjective WL after completing each experimental condition.

The Bedford technique employs a 10-element scale [38]. To address the scale loading problem associated with the NSAS-TLX technique, the Bedford scale provides detailed verbal descriptions of the 10 values on the scale. Additionally, the Bedford scale overlays a hierarchical decision tree onto the 10 WL ratings to simplify the process of selecting one of the ratings [39]. Subjects filtered their WL levels in a hierarchy, narrowing down their WL choices to two or three, and then selected a score based on the description of the rating.

(2) Work performance

It is generally accepted that increased WL affects work performance. Moreover, a large number of various kinds of literature have also validated the sensitivity and validity of performance-based measurement [40]. This study assessed work performance that reflects subjects' WL. During the experiment, the computer automatically recorded the accuracy and response time of the submersible simulated task. The ratio of accuracy and response time was used as the comprehensive performance of each subject's submersible simulated task.

(3) ECG indicators

Psychophysiological measures also provide objective WL metrics. Simulation studies have shown that the electrocardiogram (ECG) is sensitive to manipulations of task complexity [5,41]. A standard deviation of an R-R interval (SDNN), the square root of the mean squared difference of successive R-Rs (RMSSD), and a proportion of NN50 divided by the total number of NN that differ by more than 50 ms (pNN50) have been widely used as

physiological variables to measure WL in previous studies [42,43]. In this experiment, the Equivital EQ02 LifeMonitor wearable device (Cambridge, UK) was used to record ECG signals at a frequency of 250 Hz.

4.3. Experimental Procedure

In this study, a within-subjects repeated measures experimental design was employed, in which subjects were tested on six experimental conditions, labeled as Test 1–Test 6. Test 1–Test 3 represent three LOAs under LWL, and Test 4–Test 6 represent three LOAs under HWL. To reduce the effect of experimental order on the test results, each subject underwent different orders of experimental testing at each WL level using the Latin square method. This study was approved by the Institutional Review Board (IRB) of Beihang University.

Before the formal experiment, the subjects not only had sufficient training in the SBRS task but also were familiar with the task operation rules under various experimental conditions. Notably, all subjects learned to fill out the NASA-TLX scale and the Bedford scale during training. The duration of task training was 2 weeks.

Figure 4 shows the flow of the experimental test. Before the test began, the subjects wore the ECG equipment with the help of the experimenter. The experimenter introduced the next formal test process to the subjects. After adjusting the seat height and the distance between the subjects and the screen, the subjects began the formal test. The entire formal experimental test process lasted a total of 125 min and was divided into two stages. In the task testing process, subjects were asked to fill out the NASA-TLX scale and the Bedford scale after each SBRS task test. During the two SBRS task tests, subjects were prescribed a 5 min rest time. To avoid the influence of HW tests on LW tests, an additional 15 min of rest time was added when the subjects completed the two HW tests.

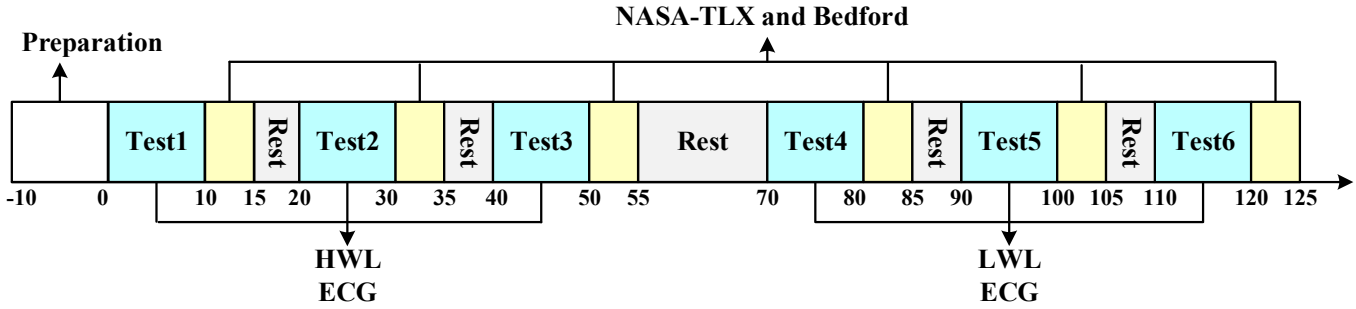

(**a**) Flow chart

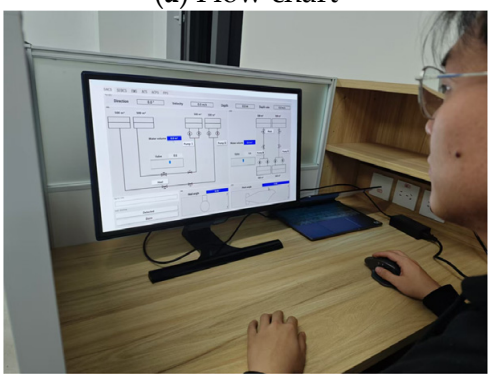

(**b**) Test chart

Figure 4. Formal experiment flow chart and test chart.

4.4. Data Analysis

The focus of this paper was to investigate whether the proposed human-machine function allocation strategy can improve the working performance of OS officers. Generalized additive mixed effect model (GAMM) analyses [33,44] were performed using the

open-source statistical package R version 3.6.1 (R Statistical Computing Project, Vienna, Austria), treating subjects as random effects. In this model, "generalized" refers to not requiring the measurement parameters y to follow a Gaussian distribution, "additive" refers to not being limited to linear relationships, and "mixed" refers to incorporating random effects. Therefore, compared with analysis of variables, GAMM analysis allows for non-linear relationships between response variables and predictor variables, and does not require measurement indicators to conform to normal distribution and homogeneity of variation conditions. In addition, this model considers subjects as random effects.

Measurement parameters used for GAMM analysis included subjective data (NASA-TLX scale data and Bedford scale data), work performance data (accuracy, response time, and comprehensive performance), and ECG data measured during task testing (SDNN, RMSSD, and pNN50). The GAMM for measuring indicators at different LOAs is shown in Equations (2) and (3):

$$y = \beta_1^1 + \beta_2^1(LOA2) + \beta_3^1(LOA3) + b^1 + e^1 \quad (2)$$

$$y = \beta_1^2 + \left(-\beta_2^2(LOA1)\right) + \beta_3^2(LOA3) + b^2 + e^2 \quad (3)$$

where, y is the specific index of the subject's response; β_1^1 and β_1^2 are the fixed intercepts; β_2^1 is the fixed effects of LOA2 compared to LOA1 at different WLs; β_3^1 is the fixed effects of LOA3 compared to LOA1 at different WLs; β_3^2 is the fixed effect of LOA3 compared to LOA2 at different WLs; b^1 and b^2 are the random effects of the intercept for subjects; e^1 and e^2 are the residuals.

5. Results

We used G*power software (latest v. 3.1.9.7) to perform statistical efficiency calculations. When setting the number of subjects to 15 and the effect size to 0.40, a significance level of 0.1 is required to achieve approximately 95% statistical power. Therefore, differences were considered statistically significant when $p < 0.1$.

5.1. Subjective WL

Figure 5 shows the impact of LOA on NASA-TLX score and Bedford score under different WLs. Under LWL, the NASA-TLX score and Bedford score for LOA1 were significantly higher than those for LOA2 and LOA3. Under HWL, the NASA-TLX score and Bedford score for LOA2 were significantly lower than those for LOA1.

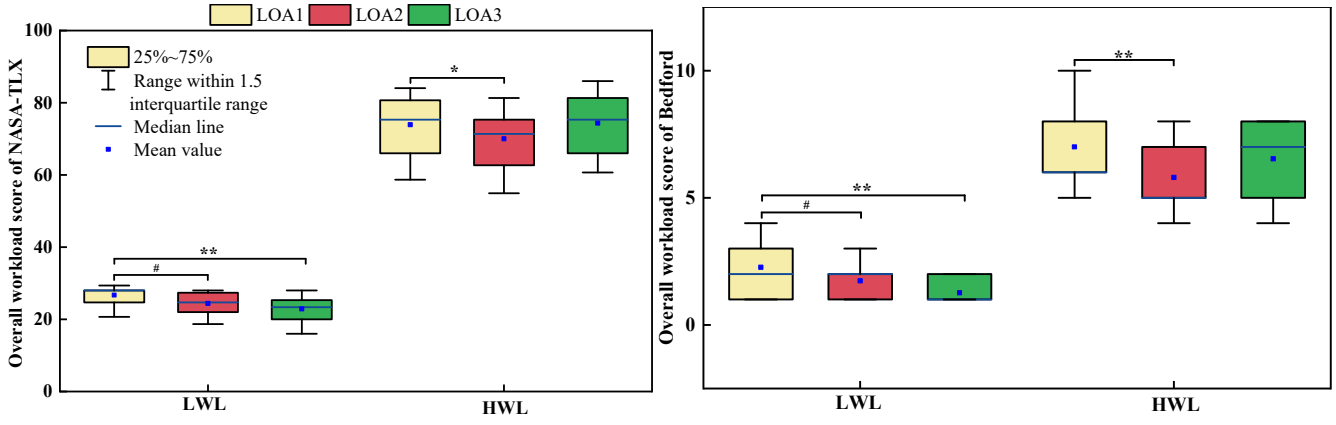

(**a**) NASA-TLX (**b**) Bedford

Figure 5. The impact of LOA on subjective WL under different WLs. # ($p < 0.1$), * ($p < 0.05$), ** ($p < 0.01$).

5.2. Work Performance

Figure 6 shows the impact of LOA on comprehensive performance, accuracy, and response time under different WLs. Figure 6a shows that under LWL, the comprehensive performance significantly increases with increasing LOA. Under HWL, the comprehensive performance for LOA2 was significantly higher than that for LOA1. As shown in Figure 6b, under LWL, the accuracy for LOA1 was significantly lower than that for LOA2 and LOA3. Under HWL, the accuracy for LOA1 was significantly higher than that for LOA2. And under LWL and HWL, the response time for LOA1 was significantly slower than that for LOA2 and LOA3 (Figure 6c).

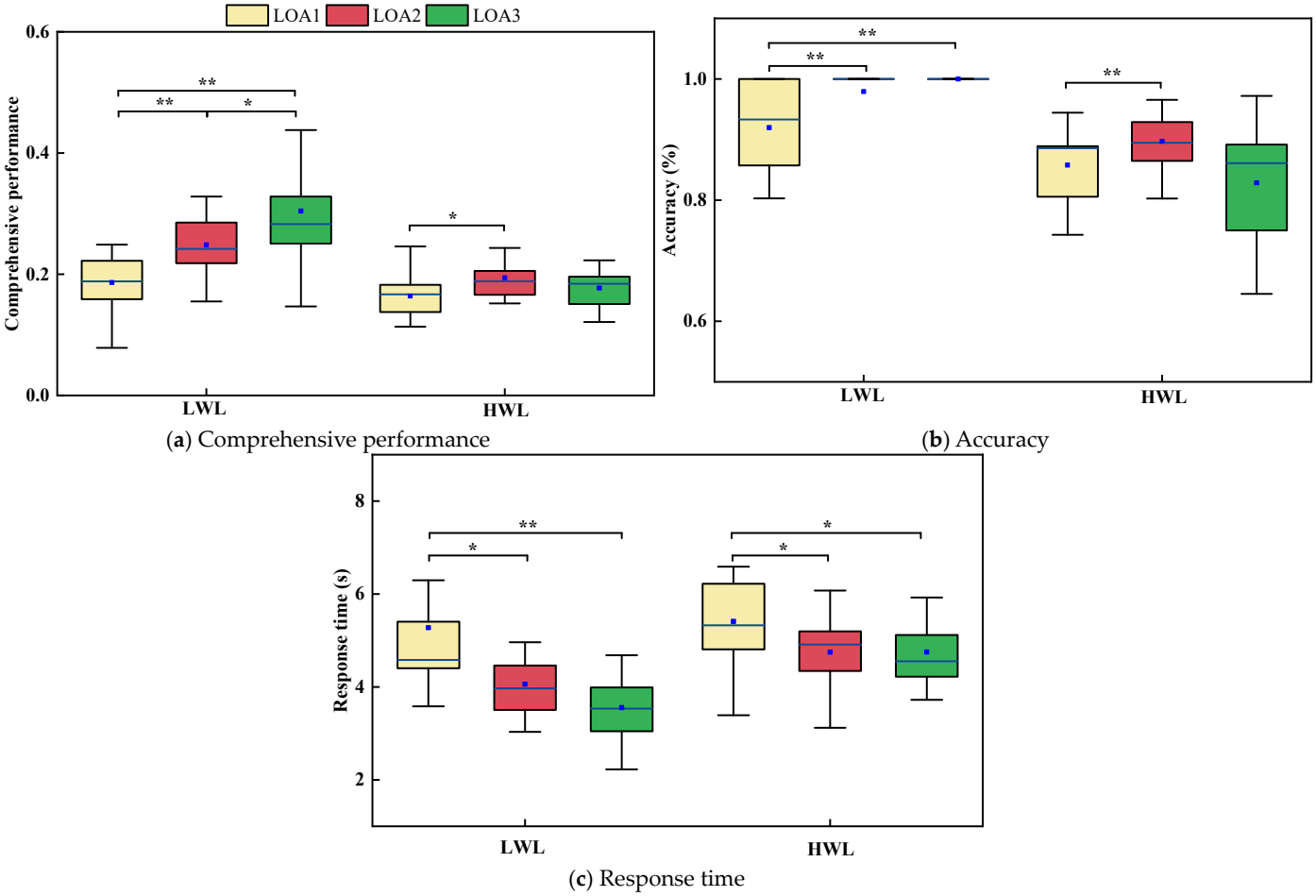

(**a**) Comprehensive performance (**b**) Accuracy

(**c**) Response time

Figure 6. The impact of LOA on work performance under different WLs. * ($p < 0.05$), ** ($p < 0.01$).

5.3. ECG Indicators

Figure 7 shows the impact of LOA on SDNN, RMSSD, and PNN50 under different WLs. Under HWL, the SDNN and the RMSSD for LOA1 were significantly lower than that for LOA2 (Figure 7a,b). The results of Figure 7c shows that LOA does not have a significant effect on SDNN and PNN50 under different WLs.

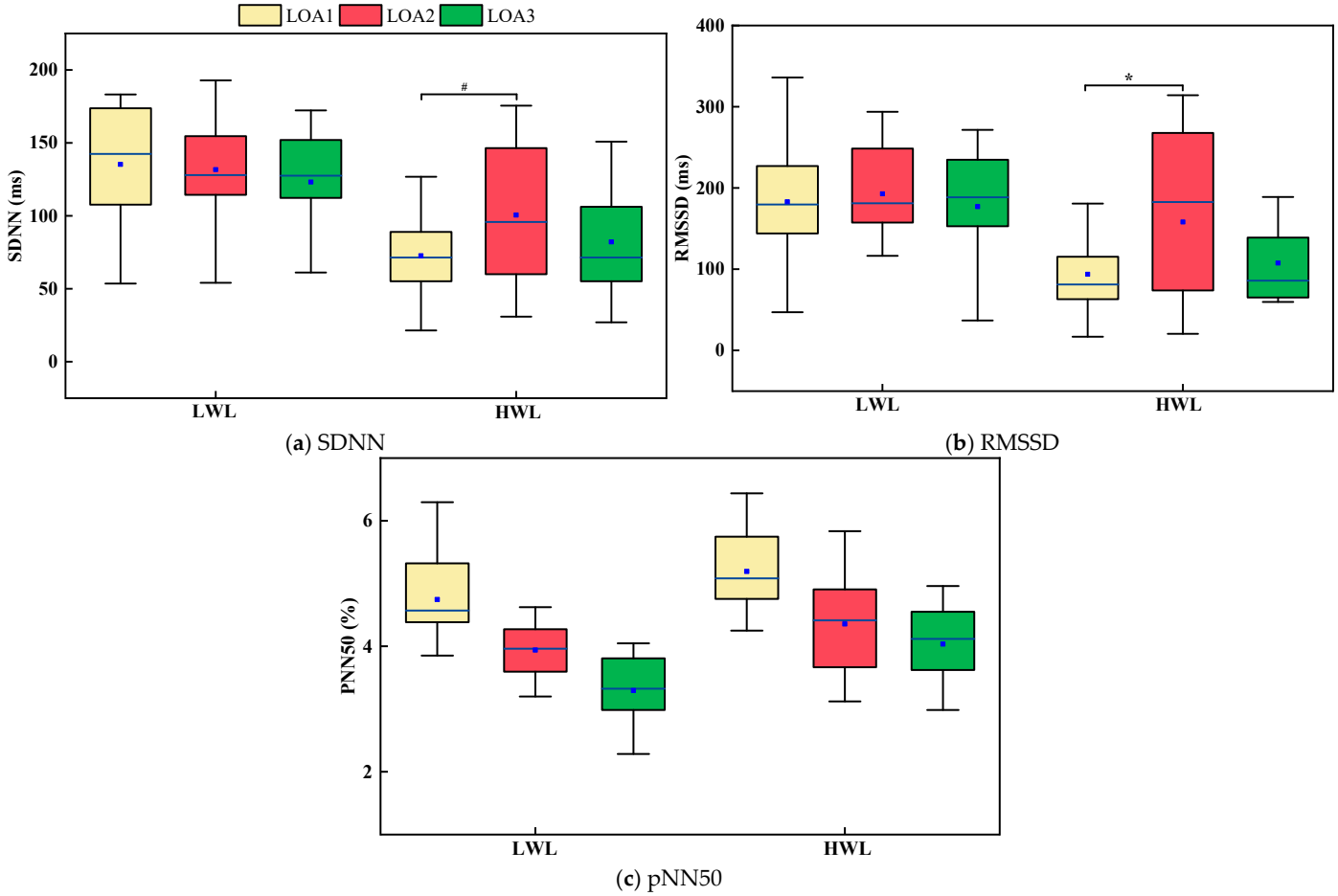

Figure 7. The impact of LOA on work performance under different WLs. # ($p < 0.1$), * ($p < 0.05$).

6. Discussions

6.1. Optimal Human-Machine Function Allocation Selection

The purpose of this paper was to investigate whether the proposed human-machine function allocation method can improve the WL and work performance of OS officers, which is mainly reflected in the impact on their subjective WL, work performance, and ECG indicators.

The results of the subjective scale indicated that LOA2 could effectively reduce the subjective WL of the subjects under HWL conditions. This indicates that machine fault detection and diagnosis during task execution can help reduce the visual search load on subjects. On the contrary, under LWL conditions, LOA3 can effectively reduce the subjective WL of subjects, but this may lead to subjects being in underload state. Therefore, LOA2 can effectively reduce the WL of subjects under HWL conditions.

Regarding the work performance of the subjects, the results showed that LOA2 significantly improved their comprehensive performance, accuracy, and response time under unbalanced WLs. LOA2 allowed subjects to focus their limited attention on fault decision-making and fault processing, which improved their attention level and reduced response time [45]. LOA3 improved comprehensive performance, accuracy, and response time under LWL, while also improving response time under HWL. Therefore, LOA2 has a positive effect on improving work performance when dealing with unbalanced WLs.

In terms of physiological status, LOA had no significant effect on SDNN and pNN50 under both HWL and LWL conditions. However, it is worth noting that LOA2 could significantly increase the RMSSD of subjects under HWL. Research has shown that an increase in RMSSD is associated with a decrease in WL [46]. Therefore, LOA2 can effectively reduce the WL of subjects under HWL.

The information filtering and integration stage of LOA3 is fully automated, and frequent pop-up interfaces can interfere with the execution of the current task. LOA3 may overly simplify human responses to dynamic tasks, potentially limiting the operator's ability to adapt to unexpected situations. LOA2 can effectively reduce WL and improve operator work performance in handling SBRS tasks under unbalanced WL conditions. Therefore, in order to achieve human-centered, human-machine collaboration, the design of human-machine function allocation must ensure that humans are the ultimate controllers of the entire system [47,48]. This study suggests that LOA2 is the optimal choice for human-machine function allocation.

6.2. Human-Machine Function Allocation in SBRS System

This study mainly proposed a new human-machine function allocation method, which successfully determined LOA2 as the optimal human-machine function allocation scheme by calculating the task complexity under different LOAs. It was experimentally verified that the proposed LOA2 can significantly improve work performance and effectively reduce WL. The conclusions drawn from this study can serve as a foundation for the design of human-machine collaboration in future submersibles, aiming to optimize work performance and reduce operator WL.

However, the introduction of automation will inevitably bring a series of risks, among which of high concern is that the addition of automation could lead to operator complacency, decreased operational skills, reduced alertness, and loss of situational awareness [25]. Therefore, in order to ensure that operators are in the human-in-the-loop throughout the human-machine interaction tasks and improve the safety and reliability, it is necessary to adopt dynamic functional allocation of the human-machine system to adapt to constantly changing resource requirements [49,50]. Our future research will focus on the dynamic functional allocation of human-machine systems.

6.3. Limitations

There are several limitations in the current research. (1) The sample sizes of the experiments were relatively small, resulting in a large variance in the experimental results of ECG data. Due to the small sample size, the statistical results were insufficient. Thus, the finding of a p-value slightly above 0.05 also deserves attention. (2) This study was unable to collect baseline physiological data from the subjects, and physiological measurement parameters were limited to electrocardiogram indicators. In future research, we will ensure the collection of baseline physiological data to evaluate more accurately the effectiveness of automated interventions. More parameters should be recommended to study how WL affects the physiological responses of subjects, such as EEG, respiratory parameters, and the electromyograph. (3) Only one of our subjects had experience working as a submersible OS officer. Thus, the results might differ from the test results of a real OS officer. However, this study carried out a 2-week training to ensure that each subject could master the task of the OS office in detail. Future studies participated by real OS officers are needed to expand the external validity of the current findings. (4) The WL in actual work scenarios is influenced by multiple factors. The STC assessment we are currently using may not cover all dimensions. In order to gain a deeper understanding of the WL of subjects in different work scenarios, we will strive to develop more comprehensive evaluation methods in future research. This will help us to more accurately grasp and interpret the WL state of the subjects in the actual work environment.

7. Conclusions

This study was devoted to improving the working performance of OS officers based on the proposed human-machine function allocation method. Three measurement techniques were used to analyze the impact of the proposed optimal human-machine function allocation on OS officers. The following conclusions were obtained through the work.

This study built a submersible SBRS system for OS officers. By analyzing the task features and task flows of the OS office, an uneven task frequency was found for the OS officer. The OS officer often faced LWL or HWL during the SBRS task. To ensure work performance, this study proposed a human-machine function allocation method based on the LOA taxonomy method and STC method. The method divided the fault handling process of OS officers into three cognitive stages and proposed three LOAs for information filtering and integration stage. Then, the task complexity of fault detection tasks under each LOA was quantified using the STC method to construct the optimal human-machine function allocation (LOA2). Finally, the experiment tests showed that LOA2 could improve the work performance and WL of OS officers during the SBRS task period under the unbalanced WL condition.

The results of this study attempt to provide a reference to allocate the human-machine function for OS officers in the future. At the same time, the method proposed in this paper can also be applied to other manned operating systems, such as aircraft, spacecraft, vehicles, and so on.

Author Contributions: Conceptualization, X.C., L.P. and C.Y.; methodology, C.Y.; software, C.Y.; validation, C.Y., L.P. and W.W.; formal analysis, C.Y. and W.W.; investigation, C.Y. and W.W.; resources, L.P. and C.Y.; data curation, C.Y.; writing—original draft preparation, C.Y.; writing—review and editing, X.C. and L.P.; visualization, C.Y.; supervision, X.C. and L.P.; project administration, X.C. and L.P.; funding acquisition, X.C. and L.P. All authors have read and agreed to the published version of the manuscript.

Funding: This research was funded by a research project (2022-JCJQ-JJ-0831), the Fundamental Research Funds for the Central Universities (JKF-20240037), and the "111 Center". The study was also supported by Beihang World TOP University Cooperation Program.

Institutional Review Board Statement: The study was conducted in accordance with the Declaration of Helsinki, and approved by the Institutional Review Board of Beihang University.

Informed Consent Statement: Informed consent was obtained from all subjects involved in the study.

Data Availability Statement: The raw data supporting the conclusions of this article will be made available by the authors on request.

Acknowledgments: The authors would like to thank all subjects involved in this study.

Conflicts of Interest: The authors declare no conflict of interest.

Appendix A

The appendix shows in detail the task complexity calculation process of ACS under LOA1. Table A1 lists the task operation process and the visual interface area corresponding to each operation behavior.

Table A1. Task decomposition of ACS.

Operation Steps	Describe	Interface Area
1	ACS Malfunction	System window
2	Click "Detected" button	Fault detection
3	Temperature specification	/
4	Check the temperature of cabins 1–10	Temperature and humidity display window
5	Determine cabin	Temperature and humidity display window
6	Report technician team	Outside interface area
7	Technician decision	Outside interface area
8	Receive fault decision results	Outside interface area
9	Click the cabin button	Operation window
10	Input decision information	Operation window
11	Click the "Done" button	Fault detection

Figure A1 shows the actions control graph of ACS. The H_{ALC} is equal to the first-order entropy of the actions control graph. The nodes of the first-order entropy in the action control graph are divided into six categories, namely {1}, {2, 3, 6, 7, 8, 9, 10}, {4.1}, {4.2, 4.3, 4.4, 4.5, 4.6, 4.7, 4.8, 4.9, 4.10}, {5}, {11}. The probabilities of each type of node are 1/20, 7/20, 1/20, 9/20, 1/20, and 1/20, respectively. The specific formula is as follows:

$$H_{ALC} = -\sum_{i=1}^{6} p(Ai)\log_2 p(Ai) = 4 \times \frac{1}{20} log_2 \frac{20}{1} + \frac{7}{20} log_2 \frac{20}{7} + \frac{9}{20} log_2 \frac{20}{9} = 1.913 \quad \text{(A1)}$$

The H_{ASC} is equal to the second-order entropy of the actions control graph. The nodes of the second-order entropy in the action control graph are divided into 20 categories, namely {1}–{11}. The probability of each stage is 1/20. The H_{ASC} value is as follows:

$$H_{ASC} = -\sum_{i=1}^{20} p(Ai)\log_2 p(Ai) = 20 \times \frac{1}{20} log_2 \frac{20}{1} = 4.322\text{A} \quad \text{(A2)}$$

Figure A2 is the interface information interaction graph. Its nodes are divided into 27 categories, namely {SACS, SUDCS}, {system window}—{11}. The probability of the first type of node is 2/28, and the probability of the remaining nodes is 1/28. The H_{IIIC} is equal to the second-order entropy of the interface information interaction graph. According to the definition of second-order entropy, the H_{IIIC} values is as follows:

$$H_{IIIC} = -\sum_{i=1}^{27} p(Ai)\log_2 p(Ai) = 26 \times \frac{1}{28} log_2 \frac{28}{1} + \frac{2}{28} log_2 \frac{28}{2} = 4.736 \quad \text{(A3)}$$

Similarly, The H_{ICBC} is equal to the second-order entropy of the information control behavior graph. As shown in Figure A3, the number of second-order entropy nodes is 12. The H_{ICBC} value is as follows:

$$H_{ICBC} = -\sum_{i=1}^{12} p(Ai)\log_2 p(Ai) = 8 \times \frac{1}{26} log_2 \frac{26}{1} + 2 \times \frac{2}{26} log_2 \frac{26}{2} + \frac{3}{26} log_2 \frac{26}{3} + \frac{11}{26} log_2 \frac{26}{11} = 1.089 \quad \text{(A4)}$$

The STC of ACS under LOA1 can be determined by the Euclidean norm. The STC value is defined as follows:

$$STC_{LOA1}^{ACS} = \sqrt{(\alpha \times H_{ALC})^2 + (\beta \times H_{ASC})^2 + (\gamma \times H_{IIIC})^2 + (\delta \times H_{ICBC})^2} \quad \text{(A5)}$$

Here, the values of α, β, γ, and δ are assumed to be 1/4 [29]. The task complexity value for the ACS is 1.823.

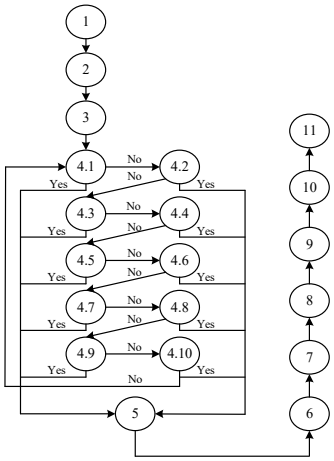

Figure A1. Actions control graph.

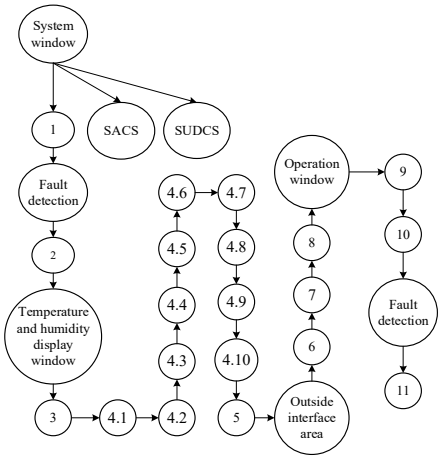

Figure A2. Interface information interaction graph.

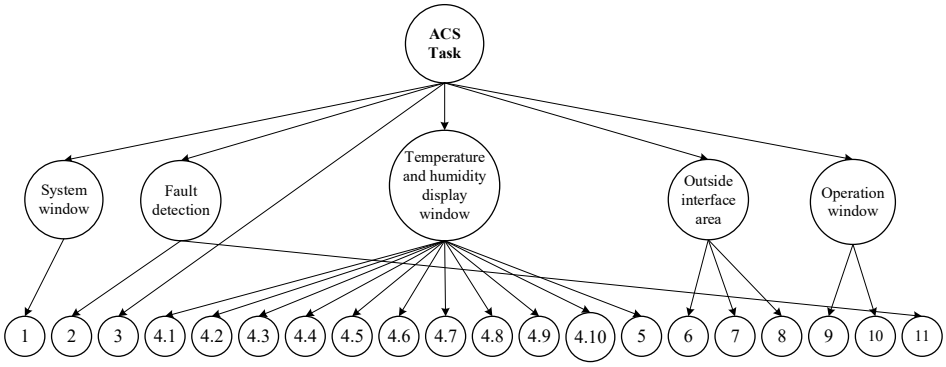

Figure A3. Interface control behavior graph.

References

1. Martin, A. Unmanned maritime vehicles: Technology evolution and implications. *Mar. Technol. Soc. J.* **2013**, *47*, 72–83. [CrossRef]
2. Zhang, T.; Tang, J.; Qin, S.; Wang, X. Review of Navigation and Positioning of Deep-sea Manned Submersibles. *J. Navig.* **2019**, *72*, 1021–1034. [CrossRef]
3. Lin, C.J.; Hsieh, T.L.; Tsai, P.J.; Yang, C.W.; Yenn, T.C. Development of a team workload assessment technique for the main control room of advanced nuclear power plants. *Hum. Factors Ergon. Manuf.* **2011**, *21*, 397–411. [CrossRef]
4. Heard, J.; Harriott, C.E.; Adams, J.A. A Survey of Workload Assessment Algorithms. *IEEE Trans. Hum.-Mach. Syst.* **2018**, *48*, 434–451. [CrossRef]
5. Hwang, S.L.; Yau, Y.J.; Lin, Y.T.; Chen, J.H.; Huang, T.H.; Yenn, T.C. Predicting work performance in nuclear power plants. *Saf. Sci.* **2008**, *46*, 1115–1124. [CrossRef]
6. Schnotz, W.; Kürschner, C. A Reconsideration of Cognitive Load Theory. *Educ. Psychol. Rev.* **2007**, *19*, 469–508. [CrossRef]
7. Song, B. A Multidimensional Workload Assessment Method for Power Grid Dispatcher. *Eng. Psychol. Cogn. Ergon.* **2018**, 55–68. [CrossRef]
8. Xie, B.; Salvendy, G. Review and reappraisal of modelling and predicting mental workload in single- and multi-task environments. *Work Stress* **2000**, *14*, 74–99. [CrossRef]
9. Cabon, P.; Coblentz, A.; Mollard, R.; Fouillot, J.P. Human vigilance in railway and long-haul flight operation. *Ergonomics* **1993**, *36*, 1019–1033. [CrossRef]
10. Wickens, C.D. Situation awareness: Review of Mica Endsley's 1995 articles on situation awareness theory and measurement. *Hum. Factors* **2008**, *50*, 397–403. [CrossRef]
11. Parasuraman, R.; Riley, V. Humans and Automation: Use, Misuse, Disuse, Abuse. *Hum. Factors* **1997**, *39*, 230–253. [CrossRef]
12. Onnasch, L.; Wickens, C.D.; Li, H.; Manzey, D. Human performance consequences of stages and levels of automation: An integrated meta-analysis. *Hum. Factors* **2014**, *56*, 476–488. [CrossRef] [PubMed]
13. Fitts, P.M.E. *Human Engineering for an Effective Air Navigation and Traffic Control System*; National Research Council: Melbourne, Australia, 1951.
14. Clegg, C.W.; Ravden, S.J.; Corbett, M.; Johnson, G.I. Allocating functions in computer integrated manufacturing: A review and a new method. *Behav. Inf. Technol.* **1951**, *8*, 175–190. [CrossRef]
15. Liu, F.; Zuo, M.; Zhang, P. Human-Machine Function Allocation in Information Systems: A Comprehensive Approach. In Proceedings of the Pacific Asia Conference on Information Systems, Brisbane, Australia, 7–11 July 2011; pp. 1–14.

16. Sheridan, T.B.; Verplank, W.L.; Brooks, T.L. Human and Computer Control of Undersea Teleoperators. In Proceedings of the 14th Annual Conference on Manual Control, Los Angleles, CA, USA, 1 November 1978.
17. Wickens, C.D. Automation Stages & Levels, 20 Years After. *J. Cogn. Eng. Decis. Mak.* **2018**, *12*, 35–41.
18. Endsley, M.R.; Kaber, D.B. Level of automation effects on performance, situation awareness and workload in a dynamic control task. *Ergonomics* **1999**, *42*, 462–492. [CrossRef]
19. Parasuraman, R.; Sheridan, T.B.; Wickens, C.D. A model for types and levels of human interaction with automation. *IEEE Trans. Syst. Man Cybern. Part A (Syst. Hum.)* **2000**, *30*, 286–297. [CrossRef]
20. Wickens, C.D. *Engineering Psychology and Human Performance*; Routledge: London, UK, 1992.
21. Kaber, D.B. Issues in Human–Automation Interaction Modeling: Presumptive Aspects of Frameworks of Types and Levels of Automation. *J. Cogn. Eng. Decis. Mak.* **2018**, *12*, 7–24. [CrossRef]
22. Endsley, M.R. Level of Automation Forms a Key Aspect of Autonomy Design. *J. Cogn. Eng. Decis. Mak.* **2018**, *12*, 29–34. [CrossRef]
23. Jamieson, G.A.; Skraaning, G. The Absence of Degree of Automation Trade-Offs in Complex Work Settings. *Hum. Factors* **2020**, *62*, 516–529. [CrossRef]
24. Wang, A.; Guo, B.; Du, H.; Bao, H. Impact of Automation at Different Cognitive Stages on High-Speed Train Driving Performance. *IEEE Trans. Intell. Transp. Syst.* **2022**, *23*, 24599–24608. [CrossRef]
25. Endsley, M.R.; Kiris, E.O. The Out-of-the-Loop Performance Problem and Level of Control in Automation. *Hum. Factors* **1995**, *37*, 381–394. [CrossRef]
26. Kaber, D.B.; Endsley, M.R. The effects of level of automation and adaptive automation on human performance, situation awareness and workload in a dynamic control task. *Theor. Issues Ergon. Sci.* **2004**, *5*, 113–153. [CrossRef]
27. Mcleod, R.W.; Walker, G.H.; Moray, N. Analysing and modelling train driver performance. *Appl. Ergon.* **2005**, *36*, 671–680. [CrossRef]
28. Ha, J.J. Development of the step complexity measure for emergency operating procedures using entropy concepts. *Reliab. Eng. Syst. Saf.* **2001**, *71*, 115–130.
29. Zheng, Y.; Lu, Y.; Wang, Z.; Huang, D.; Fu, S. Developing a Measurement for Task Complexity in Flight. *Aerosp. Med. Hum. Perform.* **2015**, *868*, 698–704. [CrossRef]
30. Shannon, C.E. A mathematical theory of communication. *Bell Syst. Tech. J.* **1948**, *27*, 623–656. [CrossRef]
31. Mowshowitz, A. Entropy and the complexity of graphs: I. an index of the relative complexity of a graph. *Bull. Math. Biophys.* **1968**, *30*, 175–204. [CrossRef]
32. Davis, J.S.; Le Blanc, R.J. A study of the applicability of complexity measures. *IEEE Trans. Softw. Eng.* **1988**, *14*, 1366–1372. [CrossRef]
33. Tao, L.; Xiao, L.; Wu, Z.; Tang, N. Automatic cognitive load classification using high-frequency interaction events: An exploratory study. *Int. J. Technol. Hum. Interact.* **2013**, *9*, 73–88.
34. Zhang, J.; Pang, L.P.; Cao, X.D.; Wanyan, X.R.; Wang, X.; Liang, J. The effects of elevated carbon dioxide concentration and mental workload on task performance in an enclosed environmental chamber. *Build. Environ.* **2020**, *178*, 106938. [CrossRef]
35. Rubio, S.; Díaz, E.; Martín, J.; Puente, J.M. Evaluation of subjective mental workload: A comparison of SWAT, NASA-TLX, and workload profile methods. *Appl. Psychol. Int. Rev.* **2004**, *53*, 61–86. [CrossRef]
36. Hart, S.G.; Staveland, L.E. Development of NASA-TLX (Task Load Index): Results of Empirical and Theoretical Research. *Adv. Psychol.* **1988**, *52*, 139–183.
37. Bandono, A.; Suharyo, O.S.R. Applied fuzzy and nasa tlx method to measure of the mental workload. *J. Theor. Appl. Inf. Technol.* **2019**, *97*, 476–489.
38. Roscoe, A.H.; Ellis, G.A. *A Subjective Rating Scale for Assessing Pilot Workload in Flight: A Decade of Practical Use*; Ministry of Defence location: Delhi, India, 1990.
39. Casner, S.M.; Gore, B.F. *Measuring and Evaluating Workload: A Primer*; National Aeronautics and Space: Washington, DC, USA, 2010.
40. Cui, X.; Zhang, Y.J.; Zhou, Y.W.; Huang, T.C.; Li, Z.Z. Measurements of team workload: A time pressure and scenario complexity study for maritime operation tasks. *Int. J. Ind. Ergon.* **2021**, *83*, 103110. [CrossRef]
41. Reinerman-Jones, L.; Matthews, G.; Mercado, J.E. Detection tasks in nuclear power plant operation: Vigilance decrement and physiological workload monitoring. *Saf. Sci.* **2016**, *88*, 97–107. [CrossRef]
42. Castaldo, R.; Melillo, P.; Pecchia, L. Acute mental stress assessment via short term hrv analysis in healthy adults: A systematic review. In Proceedings of the 6th European Conference of the International Federation for Medical and Biological Engineering: MBEC 2014, Dubrovnik, Croatia, 7–11 September 2014; Springer: Berlin/Heidelberg, Germany, 2015.
43. Zhang, J.; Cao, X.; Wang, X.; Pang, L.; Zhang, L. Physiological responses to elevated carbon dioxide concentration and mental workload during performing MATB tasks. *Build. Environ.* **2021**, *195*, 107752. [CrossRef]
44. Cao, X.; Macnaughton, P.; Cadet, L.; Cedeno-Laurent, J.; Flanigan, S.; Vallarino, J. Heart rate variability and performance of commercial airline pilots during flight simulations. *Int. J. Environ. Res. Public Health* **2019**, *16*, 237. [CrossRef]
45. Recarte, M.A.; Nunes, L.M. Effects of verbal and spatial-imagery tasks on eye fixations while driving. *J. Exp. Psychol. Appl.* **2000**, *6*, 31–43. [CrossRef]
46. Li, W.; Li, R.; Xie, X.; Chang, Y. Evaluating mental workload during multitasking in simulated flight. *Brain Behav.* **2022**, *12*, e2489. [CrossRef]

47. Billings, C.E. *Aviation Automation: The Search for A Human-Centered Approach*; CRC Press: Boca Raton, FL, USA, 1996.
48. Xing, Y.; Lv, C.; Cao, D.; Hang, P. Toward human-vehicle collaboration: Review and perspectives on human-centered collaborative automated driving. *Transp. Res. Part C Emerg. Technol.* **2021**, *128*, 103199. [CrossRef]
49. Lagu, A.V.; Landry, S.J.; Yoo, H. Adaptive function allocation stabilization and a comparison of trigger types and adaptation strategies. *Int. J. Ind. Ergon.* **2013**, *43*, 439–449. [CrossRef]
50. Ting, C.; Nassef, A.; Mahfouf, M.; Linkens, D.A.; Panoutsos, G.; Roberts, A.C. Real-time adaptive automation system based on identification of operator functional state (OFS) in simulated process control operations. *IEEE Trans. Syst. Man Cybern.-Part A Syst. Hum.* **2015**, *40*, 251–262. [CrossRef]